Int. J. Heat Mass Transfer. Vol. 24, No. 5, pp. 785–793, 1981
Printed in Great Britain

0017–9310/81/050785–08 $02.00/0
Pergamon Press Ltd

NUMERICAL STUDY OF TURBULENT DROPLET FLOW HEAT TRANSFER

SHI-CHUNE YAO and ANIL RANE*

Department of Mechanical Engineering, Carnegie-Mellon University, Pittsburgh, PA 15213, U.S.A.

(*Received* 13 *May* 1980 *and in revised form* 3 *October* 1980)

Abstract — The turbulent droplet flow heat transfer at post-dryout conditions was analyzed for the thermal entrance of circular tubes at low system pressures. The velocity and eddy diffusivity functions of Deissler [1] were used for the vapor phase, with the droplets performing as distributed heat sinks. Variable mesh was used near the wall in the numerical calculation. The analysis predicts the experimental results accurately.

NOMENCLATURE

C, wall superheat parameter;
C_p, specific heat of vapor;
d, droplet diameter;
e, thermal diffusivity for turbulent flow;
E, normalized eddy thermal diffusivity, $1 + Pr(\varepsilon_H/\nu)$;
f, friction factor;
h_d, heat transfer coefficient for evaporating droplet;
h_{fg}, latent heat of evaporation;
h_p, heat transfer coefficient of solid sphere;
k, thermal conductivity of vapor or notation for radial grid;
K_1, K_2, constants used for velocity profile or eddy diffusivity;
l, constant used for velocity profile;
m, constant used for velocity profile;
n, droplet number density;
Pr, Prandtl number of vapor;
q_w, heat flux at the wall;
r, radial position;
$\Delta r, \Delta r_1$, radial grid size for core and wall regions respectively;
R, non-dimensional radial position;
R^+, nondimensional radial position from wall;
R_1^+, non-dimensional position at interface of wall and core regions;
Re, Reynolds number;
S, heat sink parameter;
T, temperature of vapor;
T_s, saturation temperature;
u, local axial velocity;
u^+, nondimensional axial velocity profile based on u^*;
u^*, shear velocity;
U, non-dimensional form of axial velocity u/V;
V, mean axial velocity of vapor;
x, axial location;
X, non-dimensional axial location;

Greek symbols

ε_H, eddy thermal diffusivity;
η_r, non-dimensional variable in the expression of radial location;
θ, non-dimensional vapor temperature;
θ_c, non-dimensional cumulative bulk mean temperature;
μ, dynamic viscosity of vapor;
ν, kinematic viscosity of vapor;
ρ, density of fluid;
τ_w, wall shear stress;
ϕ, ratio of grid sizes at core and wall regions.

Subscripts

l, liquid;
m, bulk mean value;
0, inlet condition;
v, vapor.

INTRODUCTION

WITH the advances of numerical computation, the calculations for single phase turbulent flow heat transfer in simple geometries becomes much less difficult than before. For the thermal entrance of tubes, the predicted heat transfer matches experimental results accurately. To extend our analytical capability, this paper presents a numerical computation scheme for turbulent droplet flow heat transfer in the thermal entrance region of a circular tube. The approach used here is a natural extension of the method employed for single phase heat transfer problems. As a result, the conventional calculations of turbulent single phase heat transfer becomes a subset of this droplet flow heat transfer study.

The turbulent heat transfer of single phase flow has been calculated by Deissler [1] for the thermal entrance of circular tubes utilizing the Reynold's analogy

*Present address: Westinghouse Electric Corporation, Research and Development Center, Pittsburgh, PA 15235, U.S.A.

and integral method. A more precise calculation has been performed by Sparrow, Hallman and Siegel [2] using the method of separation of variables with the aid of numerical computation for the details of solutions. Similar methods of calculation have been extended to single phase turbulent heat transfer of more complicated flow field with reasonable success.

Turbulent heat transfer in droplet flow is of great interest to the process and energy industries with specific applications to vapor superheater, chemical processes, and nuclear reactors. However, analytical study of this problem is limited. Most of the existing analysis starts with the assumption that the heat transfer mechanisms in droplet flow can be completely decoupled and treated separately. The typical approach is the study of Koizumi, Ueda and Tanaka [3], who assumed that the flow field is one-dimensional, and heat transfer occurs between vapor and wall, droplet and vapor, and droplet and wall. The vapor-to-wall heat transfer coefficient is given by Dittus–Boelter correlation of single phase flow. The vapor-to-droplet heat transfer and droplet-to-wall heat transfer are calculated from the one-dimensional flow field. Although their analysis matches data reasonably well, this type of approach overlooks the coupling of vapor-to-wall heat transfer and vapor-to-droplet heat transfer. Practically, the coupling of these mechanisms appears in the thermal boundary layer of turbulent droplet flow which is a two-dimensional field.

As a more reasonable approach, the authors have adopted a model which considers the droplets to be distributed heat sink in the thermal field as well as dispersed vapor source in the flow field. Following this approach, the laminar heat transfer in the entrance region of circular tubes has been studied by Yao [4] considering constant droplet size and number density in the stream. More precise study of the same problem in laminar flow has been performed by Rane and Yao [5] for constant droplet size but decreasing number density along the stream due to the evaporation of droplets at low system pressures. The augmentation of heat transfer due to the presence of droplets is studied in terms of non-dimensional parameters which prescribe the dispersion of liquid phase and wall superheat respectively. This paper extends this approach to the turbulent droplet flow heat transfer. The following sections of this paper describe the fundamentals of the model, the numerical method, and the comparison of results with experimental data.

MODEL

Droplet flow heat transfer usually occurs at high void fraction. The vapor is superheated by the hot wall; however, the droplets are generally at saturation state. Since the two phase mixture is under thermally non-equilibrium state, the droplets evaporate and saturated vapor is generated in the stream.

At locations away from the tube entrance the evaporation of droplets reduces the droplet number density and increases the mean vapor velocity. The droplet size also decreases along the tube length. In many applications, the droplet flow exists at pressure very much lower than the thermodynamic critical pressure and the vapor density is much less than the liquid density. However, the latent heat of evaporation is relatively high. Under this condition the vapor generation is substantial but the change of droplet size is insignificant. As a result, the heat sink effect of the droplets decreases along the tube length mainly due to the dilution of droplet number density.

In droplet flow, heat transfer may occur between wall and vapor, wall and droplet, in addition to the thermal radiation. In this study, the post dry-out condition is considered. The wall temperature is maintained at a level higher than the 'Leidenfrost temperature' of the droplets. It has been reported by Kendall [6] that the droplet–wall contact heat transfer is negligible when wall temperature is above the Leidenfrost temperature. It has also been confirmed in the study of Koizumi, Ueda and Tanaka [3] that the droplet to wall heat transfer is much less than the vapor-to-wall or vapor-to-droplet heat transfer. Therefore, the direct contact heat transfer between wall and droplet is neglected in this study.

For many organic liquids the Leidenfrost temperature is not very high (for example, not over 350°C), therefore, the contribution of thermal radiation at such conditions can be neglected. As a result, only the wall-to-vapor and vapor-to-droplet heat transfer are to be considered in present analysis.

The droplets at the inlet of the thermal entrance region are assumed to be of the same size. In turbulent flow a droplet may move radially due to the presence of turbulence. The radial mixing of droplets over the tube cross-section makes each droplet evaporate approximately at the same rate. Hence, droplets are assumed to be of uniform size at each tube cross-section. Also due to the radial mixing, the heat sink effect of droplets in the vapor stream can be considered as homogeneous over the tube cross-section from the statistical point of view. The existence of evaporating droplets may affect the turbulent vapor flow. However, the present analysis is limited to high quality droplet flow, hence, the vapor generation per unit volume is not significant enough to distort the vapor velocity profile. Therefore, the vapor velocity profile is assumed to be the same as that of single phase turbulent flow.

Additional conditions can be assumed to further simplify the model. When the flow quality is higher than 0.5 the presence of small droplets have negligible influence on the vapor velocity profile. If the latent heat of evaporation is high, the droplet size can be assumed to be constant for reasonably long axial distance. When the chemical composition of the vapor and the droplet are identical, the mass transfer due to concentration difference will not occur. In present analysis, the variation of the vapor properties is

considered to be negligible.

In summary, the important assumptions used in present analysis are

(1) Negligible droplet-wall contact heat transfer.

(2) Negligible thermal radiative heat transfer.

(3) Uniform droplet size at the tube inlet; strong droplet mixing at downstream, single phase velocity profile.

(4) High flow quality (> 0.5) or high void fraction, constant fluid properties.

(5) Constant droplet size due to high latent heat of evaporation with significant vapor generation (a case of low pressure system). The droplets are small that the slip is negligible, and the heat transfer coefficient of droplet to vapor is a constant.

FORMULATION

The heat transfer in thermal entrance region of a tube with constant wall heat flux is studied. The coordinate system of the flow field is shown in Fig. 1. It has been reported that the evaporation at the droplet surface will reduce the heat transfer coefficient below that of an equivalent non-evaporating solid sphere [7]. The heat sink effect due to droplets can be represented in terms of the heat transferred from the superheated vapor to the saturated droplets plus the heat required to heat up the generated vapor to the vapor stream temperature. The details of the derivation of heat sink terms have been presented in Rane and Yao [5]. Therefore, the energy equation for the vapor phase can be written as

$$VU(r)\frac{\partial T}{\partial x}=\frac{1}{r}\frac{\partial}{\partial r}\left(e(r)\cdot r\frac{\partial T}{\partial r}\right)-\frac{n\pi d^2 h_p}{\rho_v C_p}(T-T_s) \quad (1)$$

where, V is the averaged vapor velocity which may increase along x due to vapor generation by droplet evaporation; $U(r)$ is the non-dimensional axial velocity profile based on V; and $e(r)$ is the thermal diffusivity of turbulent flow including molecular and eddy transport.

The initial and boundary conditions are

$$T=T_s \quad \text{at} \quad x=0 \quad (2)$$

$$\frac{\partial T}{\partial r}=0 \quad \text{at} \quad r=0 \quad (3)$$

and

$$k\frac{\partial T}{\partial r}=q_w \quad \text{at} \quad r=r_0. \quad (4)$$

Since the number of droplets passing any tube cross-section is equal to the value at the tube inlet, the local mean vapor velocity can be related to the local droplet number density as

$$Vn=V_0 n_0. \quad (5)$$

The variation of droplet number density can be related to the change of droplet size as

$$\rho_l n\pi d^2 \tfrac{1}{2}\,\mathrm{d}d=\rho_v\frac{\mathrm{d}n}{n}. \quad (6)$$

Again, the evaporation rate of the droplet can be expressed in terms of the change in droplet diameter with time or position as

$$\pi d^2 h_d(T_m-T_s)=-\tfrac{1}{2}\rho_l h_{fg}\pi d^2\frac{\mathrm{d}d}{\mathrm{d}x}V \quad (7)$$

where $\mathrm{d}d$ denotes the incremental change in droplet diameter, and T_m is used for the average heat transfer to droplets. The use of T_m in this equation is consistent with the assumption (3) of strong mixing of droplets at any cross-section. The approximation was made here that the droplet velocity is very close to the vapor velocity when droplets are small. From equations (5), (6) and (7) the droplet density is obtained as a function of axial distance x. The result is

$$\frac{1}{n^2}=\frac{1}{n_0^2}+\frac{2\pi d_0^2 h_p}{\rho_v h_{fg} V_0 n_0}\int_0^x\frac{T_m-T_s}{1+C_p(T_m-T_s)/h_{fg}}\mathrm{d}x \quad (8)$$

where the bulk mean temperature is defined as

$$T_m=\frac{2}{r_0^2}\int_0^{r_0}TU(r)r\,\mathrm{d}r. \quad (9)$$

With equations (5) and (8), the description of equation (1) is complete. This set of equations can be non-dimensionalized in terms of

$$R=(r/r_0) \quad (10)$$

$$X=(x/r_0)/RePr \quad (11)$$

and

$$\theta=k(T-T_s)/q_w r_0 \quad (12)$$

where,

$$Re=2V_0 r_0/\nu \quad (13)$$

and

$$Pr=\mu C_p/k. \quad (14)$$

The resulting set of equations is

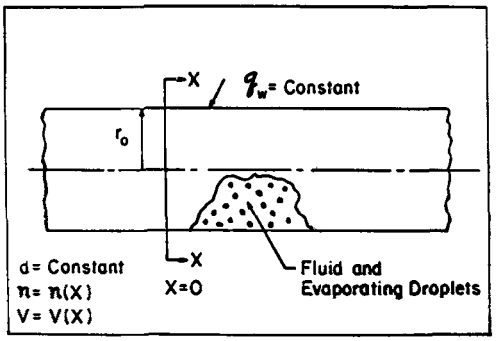

FIG. 1. Evaporating droplet flow in a circular tube.

$$\tfrac{1}{2}[1+4S\theta_c]^{1/2}\,U(R)\frac{\partial\theta}{\partial X} = \frac{1}{R}\frac{\partial}{\partial R}\left(E(R)R\frac{\partial\theta}{\partial R}\right) - \frac{S\theta}{[1+4S\theta_c]^{1/2}} \quad (15)$$

with initial and boundary conditions

$$\theta = 0 \text{ at } x = 0 \quad (16)$$

$$\frac{\partial\theta}{\partial R} = 0 \text{ at } R = 0 \quad (17)$$

$$\frac{\partial\theta}{\partial R} = 1 \text{ at } R = 1. \quad (18)$$

In equation (15) the parameters are defined as follows

$$S = \pi n_0 d_0 r_0^2 \left\{\frac{h_p d_0}{k}\right\} \quad (19)$$

is the sink parameter defined on inlet condition,

$$\theta_c = \int_0^x \frac{\theta_m}{(1/C)+\theta_m}\,dx \quad (20)$$

is the cumulative bulk mean temperature with

$$C = C_p q_w r_0/kh_{fg} \quad (21)$$

as the wall superheat parameter, and

$$\theta_m = 2\int_0^1 \theta U(R)R\,dR \quad (22)$$

as the bulk mean vapor temperature.

Non-dimensional velocity and eddy diffusivity functions $U(R)$ and $E(R)$ are derived from expressions suggested by Deissler [1], and can be expressed as follows

$$U(R) = mRe_e^{-l}\left[u_1^+ + \frac{1}{K_1}\ln\left(\frac{R^+}{R_1^+}\right)\right] \quad \text{for } R^+ > R_1^+ \quad (23)$$

$$= mR_e^{-l}\int_0^{R^+}\frac{dR^+}{1+K_2u^+R^+[1-\exp(-K_2u^+R^+)]} \quad \text{for } R^+ \leqslant R_1^+ \quad (24)$$

$$E(R) = 1 + Pr(K_1RR^+ - 1) \quad \text{for } R^+ > R_1^+ \quad (25)$$

$$E(R) = 1 + Pr[K_2u^+R^+[1-\exp(-K_2u^+R^+)]] \quad \text{for } R^+ \leq R_1^+ \quad (26)$$

with

$$K_1 = 0.36 \quad (27)$$

$$K_2 = 0.01537 \quad (28)$$

$$R_1^+ = 26 \quad (29)$$

$$u_1^+ = 12.84 \quad (30)$$

$$\left.\begin{aligned} m &= 0.19875 \\ l &= 0.125 \end{aligned}\right\} \text{ for } 5000 < Re \leq 30\,000 \quad (31), (32)$$

$$\left.\begin{aligned} m &= 0.15166 \\ l &= 0.10 \end{aligned}\right\} \text{ for } 30\,000 < Re \leq 1\,000\,000. \quad (33), (34)$$

The non-dimensional velocity and radial position are defined as

$$u^+ = u/u^* \quad (35)$$

and

$$R^+ = (1-R)\eta_r \quad (36)$$

where

$$u^* = (\tau_w/\rho_v)^{1/2} \quad (37)$$

$$\eta_r = r_0u^*/v. \quad (38)$$

The evaluation of the shear velocity u^* depends upon the wall stress which can be evaluated from

$$\tau_w = f\tfrac{1}{2}\rho_v V^2 \quad (39)$$

with friction factor calculated from

$$f = 0.079Re^{-0.25} \quad \text{for } 5\times10^3 < Re \leq 3\times10^4 \quad (40)$$

and

$$f = 0.046Re^{-0.20} \quad \text{for } 3\times10^4 < Re \leq 10^6. \quad (41)$$

NUMERICAL METHOD

The finite difference scheme is used with a downstream marching procedure. The grid system used in numerical calculation is shown in Fig. 2. In the X-direction the axial increment is selected within the range 10^{-4}–10^{-5}. In the R-direction variable grid is used because the turbulent velocity and temperature profiles vary sharply near the wall. From the centerline to the location where R equals 0.9, a coarse radial increment of 2.5×10^{-1} is used. From this point till the wall, the radial increment is selected within the range 2.5×10^{-3}–0.625×10^{-3}. Generally, fine increments are used when Reynolds number or Prandtl number of the vapor stream is high.

At the location where grid size changes, a fictitious point has to be assigned to evaluate the radial derivative at that joining point. As indicated in Fig. 2, at an axial position i the radial grid size changes at the location k. The temperature at point p is determined by passing a parabola through the temperatures at points $k+1$, k and $k-1$ and then performing interpolation. As a result

$$\theta_{i,p} = \left[\frac{2\phi^2}{1+\phi}\right]\theta_{i,k-1} + 2(1-\phi)\theta_{i,k} + \left[\frac{\phi-1}{\phi+1}\right]\theta_{i,k+1} \quad (42)$$

where

$$\phi = \Delta r_1/\Delta r.$$

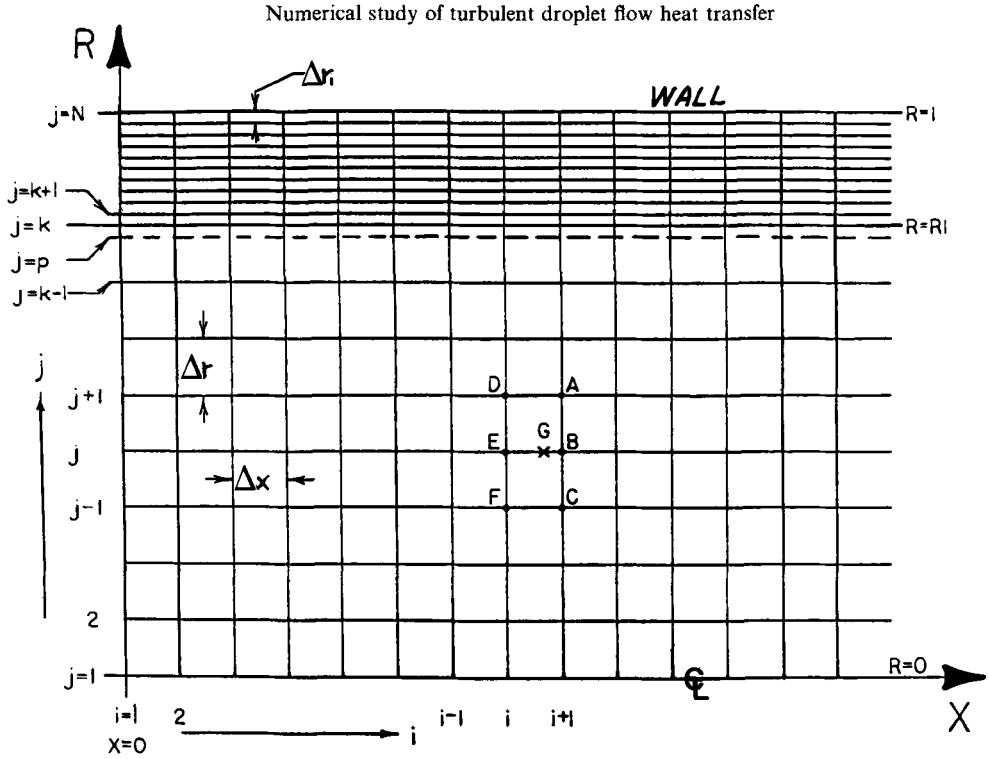

FIG. 2. Finite difference grid superimposed over the rectangular representation of the region defined by $R = 0$, $R = 1$ and R-axis.

It is well known that by writing the governing equations in finite difference form, the explicit scheme may lead to stability problems. In this study, a general representation is chosen to allow for arbitrary selection of the degree of implicitness. The resulting difference equation is a linear combination of an explicit scheme with weighing factor $(1 - \lambda)$ and an implicit scheme with weighing factor λ. The range of λ is between 0 to 1 and the scheme is universally stable when λ is in the range of 0.5–1.0. In these calculations λ is set to 1.00.

At the centerline, the boundary condition is used with forward difference representation of the order of Δr^2. At the wall a backward difference representation of the order of Δr_1^2, is used. The resulting system of equations for temperature is put into a matrix form. Through a few adjustments, it can be reduced to a tridiagonal form and solved with the Gauss elimination method. The mean vapor temperature is evaluated using Simpson's rule which is a fourth-order numerical integration method. The cumulative mean vapor temperature is then evaluated using a second-order trapezoidal rule for numerical integration.

The numerical computation is performed on a DEC-20 computer. Typically, the CPU time required to perform calculation for one axial step with the mesh size described previously is 5 s. To compare with the experimental data of Koizumi, Ueda and Tanaka [3], 60 axial steps are required.

RESULTS AND DISCUSSION

The limiting case of turbulent droplet flow heat transfer calculation is the single phase flow where no droplets are present in the stream and therefore the heat sink effect disappears from the vapor stream. For the turbulent single phase flow in the thermal entrance region, the analysis has been performed by Sparrow, Hallman and Siegel [2]. The computed results of this study match the calculated results of Sparrow, Hallman and Siegel satisfactorily.

There have been many experimental efforts to understand turbulent droplet flow heat transfer. However, most of the reported data cannot be used here for comparison with the calculated results of the present study. In order to adequately describe the condition of a droplet flow, the liquid mass flow as well as the size of droplets must be reported. The measurement of droplet size in a droplet flow, however, has been seldom performed in most experiments, due to its inherent difficulty. To the knowledge of the authors, only the experiments of Koizumi, Ueda and Tanaka [3] reported all the pertinent information completely. In their test the droplets are sampled and measured. The test section is heated with constant heat flux and the local wall temperatures are reported. The working fluid is Freon-113.

Table 1. Basic parameters for comparison with Koizumi, Ueda and Tanaka's experimental data

Experimental data from [3] (tube radius $r_0 = 5$ mm)					Corresponding parameters from present analysis					
Figure no. in [3]	P_s, bar	Q_w, W m^{-2}	$\dot{M}_{l0}$, kg h^{-1}	$\dot{M}_{g0}$, kg h^{-1}	d_0, μm	Re_0	$\overline{Re}$	Pr	S	A	C
3	3.08	2.13×10^4	76.7	177	30	5.5×10^5	7.9×10^5	0.8	2165	0.433	52
4	3.08	8.41×10^4	86.3	165	30	5.1×10^5	7.8×10^5	0.8	2615	0.523	207
5	3.09	7.14×10^4	57.5	164	30	5.1×10^5	6.9×10^5	0.8	1755	0.351	176

Calculations are performed to compare analytical results with the data of Koizumi, Ueda and Tanaka [3]. The initial conditions for the experimental data and corresponding parameters for the present analysis are given in Table 1. In their tests there is always a wet length of the tube at the upstream of the dryout zone. However, the present calculation for turbulent droplet flow heat transfer starts at dryout point. Therefore, only the results in the dryout zone are calculated for comparison. The starting point of the dryout zone of each test can be identified easily from the location where the wall temperature data starts to rise sharply.

The typical comparisons are presented here for the cases of the lowest heat flux (Fig. 3), a medium heat flux (Fig. 4) and the highest heat flux (Fig. 5). In Figs. 3 and 4 the predicted wall temperature follows the data closely with the largest difference of about 10% for downstream. The comparison in Fig. 5 is very encouraging. The present calculations predict the data within the range of its scatter.

It is important to point out that the present calculation follows a rigorous model and method. Therefore, the agreement of the prediction with the data gives strong confidence in the accuracy of both the model and the method of calculation. Also included in the Figs. 3, 4 and 5 are the wall temperature variations for the single phase flow with the same mass flow rate. In the droplet flow, the Reynolds number of the vapor field approaches gradually to the Reynolds number of this single phase flow which corresponds to the condition where all the droplets are evaporated completely. The discrepancy is apparent especially for the condition of high heat flux. This implies the necessity of applying a droplet flow heat transfer model instead of a single phase heat transfer approximation.

CONCLUSION

In this paper, a model for turbulent droplet flow heat transfer in circular tubes is proposed which considers the coupled effects of droplet-to-vapor and vapor-to-wall heat transfer. The heat transfer effect of droplets is considered as a heat sink in the vapor stream. The model is developed and the method of calculation is illustrated. The model predicts the experimental results for turbulent droplet flow heat transfer with constant wall heat flux accurately. The model also confirms the existing analytical result for single phase turbulent flow heat transfer in circular tubes. It is possible that this approach may be applied to more complicated turbulent droplet flow heat transfer problems with reasonable success.

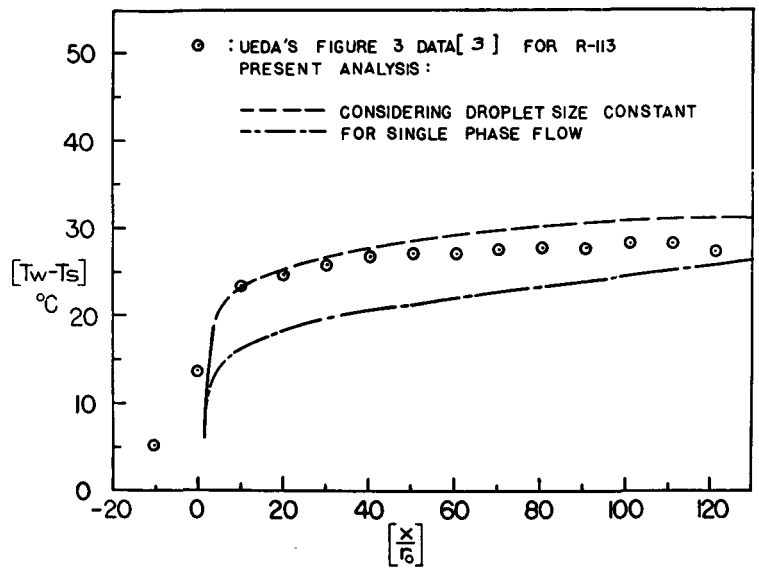

FIG. 3. Comparison of dispersed flow heat transfer results with experimental data. $S = 2165$, $A = 0.433$, $C = 52$ and $Re_0 = 5.5 \times 10^5$, $Pr = 0.8$.

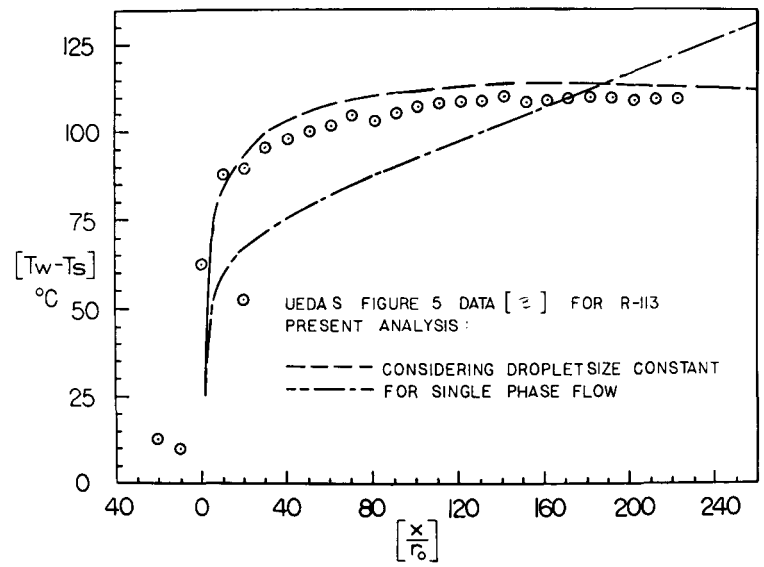

FIG. 4. Comparison of dispersed flow heat transfer results with experimental data. $S = 1755$, $A = 0.351$, $C = 176$ and $Re_0 = 5.1 \times 10^5$, $Pr = 0.8$.

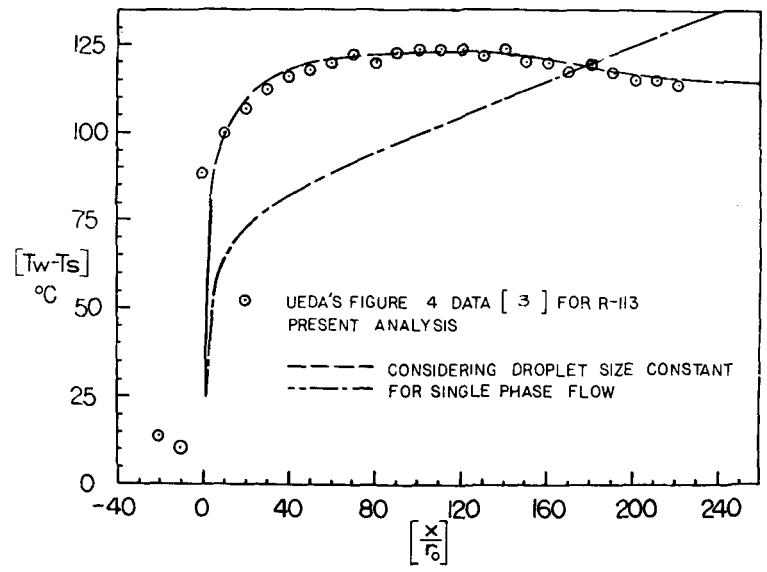

FIG. 5. Comparison of dispersed flow heat transfer results with experimental data. $S = 2615$, $A = 0.523$, $C = 207$ and $Re_0 = 5.1 \times 10^5$, $Pr = 0.8$.

REFERENCES

1. R. G. Deissler, Analysis of turbulent heat transfer, mass transfer, and friction in smooth tubes at high Prandtl and Schmidt numbers. NACA Report 1210, Washington, D.C. (1955).
2. E. M. Sparrow, T. M. Hallman and R. Siegel, Turbulent heat transfer in the thermal entrance region of a pipe with uniform heat flux. *Appl. Sci. Res.* **7A**, 37–52 (1957).
3. Y. Koizumi, T. Ueda and H. Tanaka, Post dryout heat transfer to R-113 upward flow in a vertical tube, *Int. J. Heat Mass Transfer* **22**, 669–678 (1979).
4. S. C. Yao, Convective heat transfer of laminar droplet flow in thermal entrance region of circular tubes. *J. of Heat Transfer, Trans. ASME* **101**(3), 480–483 (1979).
5. A. Rane and S. C. Yao, Heat transfer of evaporating droplet flow in low pressure systems. *Canad. J. Chem. Engng* **58**(3), 303–308 (1980).
6. G. E. Kendall, Heat transfer to impacting drops and post critical heat flux dispersed flow. Ph.D. Thesis, M.I.T. (1978).
7. M. C. Yuen and L. W. Chen, Heat transfer measurements of evaporating liquid droplets. *Int. J. Heat Mass Transfer* **21**, 537–542 (1978).

ETUDE NUMERIQUE DU TRANSFERT THERMIQUE DANS L'ECOULEMENT TURBULENT DE GOUTTELETTES

Résumé — On analyse l'écoulement turbulent de gouttelettes dans les conditions d'assèchement de la paroi, à l'entrée des tubes circulaires et pour des faibles pressions. Les lois de vitesse et de diffusivité turbulente de Deissler [1] sont utilisées pour la phase vapeur et les gouttelettes sont considérées comme des puits de chaleur distribués. On utilise près de la paroi des mailles variables pour le calcul numérique. L'analyse approche correctement les résultats expérimentaux.

NUMERISCHE UNTERSUCHUNG DES WÄRMEÜBERGANGS BEI TURBULENTER TRÖPFCHENSTRÖMUNG

Zusammenfassung—Der Wärmeübergang bei turbulenter Tröpfchenströmung im post-dryout-Gebiet wurde für den thermischen Einlauf von Rohren bei niederen Systemdrücken theoretisch untersucht. In der Dampfphase wurden die Ansätze von Deissler [1] für Geschwindigkeit und turbulenten Transport verwendet — die Tröpfchen wirken als verteilte Wärmesenken. Bei der numerischen Berechnung wurde nahe der Wand variable Maschenweite verwendet. Der theoretische Ansatz gibt die experimentellen Ergebnisse genau wieder.

ЧИСЛЕННОЕ ИССЛЕДОВАНИЕ ТЕПЛООБМЕНА ПРИ ТУРБУЛЕНТНОМ ТЕЧЕНИИ ГАЗО-ЖИДКОСТНОГО ПОТОКА

Аннотация — Анализируется теплообмен в турбулентном двухфазном (газ-капли жидкости) потоке при закритических условиях на начальном тепловом участке круглых труб при низких давлениях. Для газо-образной фазы используются функции скорости и турбулентной температуропроводности Дейсслера [1]; при этом капли играют роль рассредоточенных полотителей тепла. При проведении численного расчета у стенки была использована сетка с переменным шагом. Результаты анализа достаточно хорошо соответствуют экспериментальным данным.